JOURNAL OF SOLID STATE CHEMISTRY 27, 201–207 (1979)

The Ionic Conductivity of PbFBr

A. F. HALFF

Physical Laboratory, Solid State Chemistry Department, State University, P.O. Box 80.000, 3508 TA Utrecht, The Netherlands.

Received March 20, 1978; in revised form May 22, 1978

The ionic conductivity of undoped and doped PbFBr crystals is reported. Measurements were performed parallel and in some instances perpendicular to the crystallographic c-axis. Furthermore, results on aliovalent doped pressed pellets are presented. The influence of inevitably present oxygen impurities and deviations from molecularity is discussed in conjunction with the role of deliberately added aliovalent metal halides. In accordance with a model developed for PbFCl the mechanisms of mass transport in PbFBr are proposed and related with observed conductivity activation enthalpies.

1. Introduction

To date no detailed studies of the electrical properties of lead fluorobromide have been reported in the literature. From transference number measurements it has been established that mixed anionic conduction with $t_{F^-} = 1 - t_{Br^-} = 0.87$ prevails in the temperature range 523–573°K (*1*).

PbFBr is isostructural with tetragonal PbFCl, and has a unit cell with layer sequence F Pb Br Br Pb F (*2*). For both these ternary halides it has been established that the ionic conductivity is anisotropic (*3*).

The melt growth of the ternary lead fluorohalides PbFX (X = Cl, Br) leads in general to the compositions $PbF_{1-x}X_{1+x}$ or $PbF_{1+x}X_{1-x}$ with $x \neq 0$ (*3, 4*). A separate phase of one of the binary constituents may even be present. The deviations from molecularity affect the concentrations of the ionic point defects, and hence the ionic conductivity. It has been proposed that the dissolution of one of the binary constituents in, for instance, PbFBr enhances the concentrations of lead ion vacancies, and of either fluoride or bromide ion vacancies. In addition it has been established that PbFBr in equilibrium with bromine gas remains stoichiometric (*3*).

In order to characterize the mass transport processes in PbFBr in more detail, the ionic conductivity of undoped crystals, and of crystals doped with aliovalent metal halides has been studied parallel and in several instances perpendicular to the crystallographic c-axis. Measurements were performed also on polycrystalline compacts.

In view of the great similarity between the crystal structure of and the mobile ions in PbFBr and PbFCl the present data for PbFBr will be discussed using the mechanisms for ionic transport which have been developed for PbFCl. Moreover, the role of oxygen impurities will be discussed.

2. Experimental

In this study single crystals or polycrystalline compacts were investigated. The crystals were grown from a melt consisting of an equimolar mixture of PbF_2 and $PbBr_2$ plus up to about 10% excess by weight of $PbBr_2$.

0022-4596/79/020201-07$02.00/0

Details of the growth procedure have been published elsewhere (*4*). Doping with silver and lanthanum was performed by adding silver bromide (Optran), silver fluoride (Merck), or lanthanum fluoride (Koch–Light) before zone melting. The single crystals were cleaved from the crystalline parts of the ingot and had surface areas up to 0.4 cm^2, and a thickness of about 0.1 cm. The diameter of the used compacts was 0.86 cm, while thicknesses varied from 0.1 to 0.3 cm. The compacts were obtained by sintering powders of the polycrystalline part of the ingot for 60 hr at about 620°K in a purified nitrogen ambient to improve the density.

Spectrographic analysis of undoped PbFBr crystals revealed the presence of cationic impurities in the concentration region 5 to 60 weight ppm (*5*). Analyses of samples deliberately doped with about 300 ppm dopant revealed that only small amounts of the dopant had actually been dissolved. In PbFBr crystals doped with AgBr, for example, the largest amount detected was about 50 ppm Ag by weight. Large amounts of the dopants were found in the polycrystalline parts of the zone-refined AgF-doped material, viz. 680 weight ppm Ag. Conductivity results show that this material was not single phase.

The experimental set-up for the a.c. conductivity measurements has been published before (*3*). In addition admittance parameters of PbFBr ($\perp$ and $\parallel$ c-axis) between ionically blocking platinum paste electrodes (Leitplatin, Degussa) were recorded in the range 10^{-2} Hz–10 kHz using a Solartron Frequency Response Analyzer (1170). Complex-plane analysis of the frequency dispersion revealed the low-frequency intercept to be at the origin of the admittance plot indicating negligible electronic conductivity. The data presented in this paper were measured usually at the constant frequency of 10 kHz, and represent bulk conductivities. The ambient was dry, purified nitrogen.

3. Results

In Fig. 1 we have gathered representative examples of the temperature dependence of the ionic conductivity of undoped PbFBr crystals. Curves 1, 2 and 3 reveal a conductivity anomaly which starts at about 620°K in the case of curves 1 and 3. Figure 2 represents the data for crystals doped with AgBr and their undoped starting materials. The data reveal that upon doping with AgBr the conductivity decreases over the entire extrinsic region with respect to undoped crystals. In Fig. 3 we have plotted the data of LaF_3- doped materials and their undoped starting materials. The ionic conductivity parallel to the c-axis of the LaF_3-doped crystals is found in the same region as that of the undoped starting materials. Suitable, undoped crystals for measurements perpendicular to the c-axis could not be cleaved from the zone-refined $PbBr_2$ rich ingots. Therefore, the influence of doping with LaF_3 on the conductivity perpendicular to the c-axis could not be evaluated. It is evident from the data presented in Fig. 3 that the conductivity of PbFBr is anisotropic. The polycrystalline PbFBr : AgBr samples exhibited an ionic conductivity lower than that of

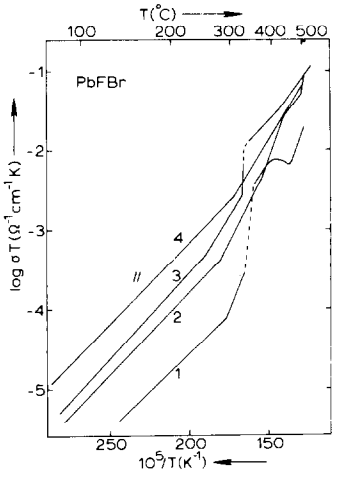

FIG. 1. The ionic conductivity of undoped PbFBr crystals measured parallel to the c-axis.

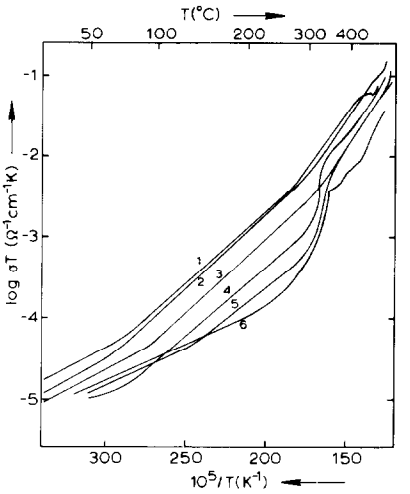

FIG. 2. The ionic conductivity of PbFBr crystals doped with AgBr (4–6) and their undoped starting material (1–3). Crystals were measured parallel to the c-axis. The sequence 4–6 indicates an increasing amount of dopant.

the undoped material, i.e. in accordance with the data for crystals presented in Fig. 2.

The polycrystalline AgF-doped material showed a different behavior (see Fig. 4). Up to about 400°K the conductivity is independent of the sample studied, having a conductivity activation enthalpy of (0.59 ± 0.03) eV,

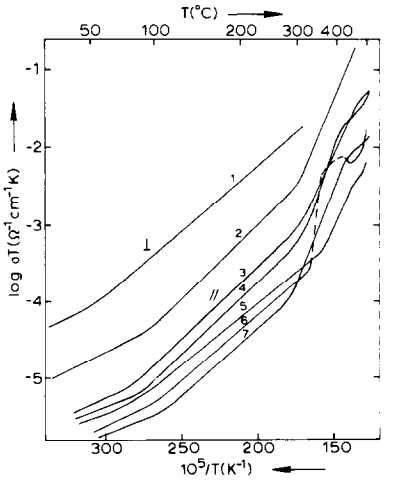

FIG. 3. The ionic conductivity of PbFBr doped with LaF_3 (1, 2: ⊥ c-axis; 4, 5: ∥ c-axis) and their undoped starting material (3, 6 and 7).

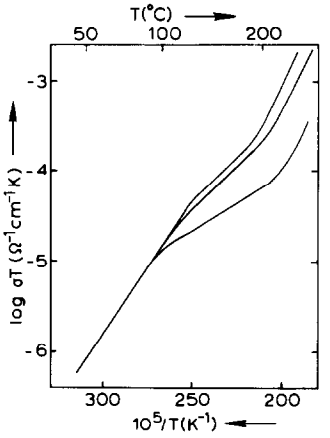

FIG. 4. The low-temperature ionic conductivity of pressed pellets of PbFBr doped with AgF for three different samples from one and the same batch.

while above this temperature the conductivity depends on the sample. This indicates the presence of AgF as a separate phase.

In Table I we have summarized the conductivity activation enthalpies. The sequence $\Delta H_1 \rightarrow \Delta H_3$ indicates data from low to high temperatures. The method of data analysis is the same as described before for PbFCl (*6*).

4. Discussion

Just as in PbFCl, mixed anionic conductivity prevails in PbFBr at elevated temperatures (*1*). Together with structural considerations, this behavior indicates that the intrinsic disorder in PbFBr is of the Schottky type, i.e.

$$Pb_{Pb}^{\times} + F_F^{\times} + Br_{Br}^{\times} \rightleftarrows V_{Pb}'' + V_F^{\cdot} + V_{Br}^{\cdot} + (PbFBr)_{defect} \quad (1)$$

where $(PbFBr)_{defect}$ stands for a lattice unit situated at a one- or more dimensional lattice defect.

The extrinsic conductivities of the ternary lead halides are governed by the extent to which solid solution formation has occurred, and by the presence of oxygen impurities (*3, 7*). The main source of oxygen impurities

TABLE I

CONDUCTIVITY ACTIVATION ENTHALPIES FOR UNDOPED AND DOPED PbFBr SAMPLES

	ΔH_1 (eV)	ΔH_2 (eV)	ΔH_3 (eV)	Data (Fig.)
PbFBr ($\parallel$ c-axis)	—	0.36 ± 0.04	0.9 ± 0.1	1
PbFBr ($\parallel$ c-axis)	0.12 ± 0.02	0.36 ± 0.04	0.7 ± 0.1	2
PbFBr ($\parallel$ c-axis)	0.10 ± 0.02	0.38 ± 0.04	0.9 ± 0.1	3
PbFBr:AgBr ($\parallel$ c-axis)	0.13 ± 0.02	0.36 ± 0.04	—	2
PbFBr:LaF_3 ($\parallel$ c-axis)	0.10 ± 0.02	0.37 ± 0.04	0.9 ± 0.1	3
PbFBr:LaF_3 ($\perp$ c-axis)	0.15 ± 0.02	0.41 ± 0.04	1.1	3
PbFBr (p.c)	0.12	0.40	1.3	—
PbFBr:AgBr (p.c)	0.10	0.38	1.3	—

is the binary constituent β–PbF_2 used in the melt growth of PbFX (X = Cl, Br) (*7*), although it has been well established that even zone refined PbX_2 contains PbO (*8*).

In general $PbBr_2$ rich solid solutions are formed during melt growth, (*3*) the excess $PbBr_2$ being dissolved according to

$$PbBr_2 \rightarrow Pb_{Pb}^{\times} + V_{Pb}'' + 2V_F^{\cdot} + 2Br_{Br}^{\times}. \quad (2)$$

Conductivity anomalies starting at about 620°K have been attributed to melting of a $PbBr_2$ rich eutectic composition which is present as a separate phase (*3*).

Oxygen impurities enter the PbFBr lattice as PbO, Al_2O_3 and/or SiO_2 (*5*, *7*). The ionic radii involved indicate a preference for substitutional replacement of fluoride ions by oxide ions. The lattice reactions involved can, therefore, be described by

$$PbO \rightarrow Pb_{Pb}^{\times} + O_F' + V_{Br}^{\cdot} \quad (3)$$

$$Al_2O_3 \rightarrow 2Al_{Pb}^{\cdot} + 2O_F' + O_{Br}' + V_{Br}^{\cdot}, \quad (4)$$

or

$$Al_2O_3 \rightarrow 2Al_{Pb}^{\cdot} + V_{Pb}'' + 3O_F' + 3V_{Br}^{\cdot} \quad (5)$$

$$SiO_2 \rightarrow Si_{Pb}^{\cdot\cdot} + O_F' + O_{Br}' \quad (6)$$

or

$$SiO_2 \rightarrow Si_{Pb}^{\cdot\cdot} + V_{Pb}'' + 2O_F' + 2V_{Br}^{\cdot}. \quad (7)$$

These types of oxygen impurities give (apart from (6)) rise to an extrinsic concentration of bromide ion vacancies.

It has been shown (*3*) that the extrinsic conductivities of PbFCl in which at high temperatures premelting effects occur can be used to determine whether oxygen impurities or deviations from molecularity predominate. A similar situation is found in Fig. 1. The extrinsic conductivity decreases when an increasing deviation from molecularity is encountered. In view of equilibrium (1) and reaction (2) the bromide ion vacancy concentration decreases with increasing amount of dissolved $PbBr_2$. The bromide ion vacancy concentration thus fixed would, however, be strongly temperature dependent, contrary to the data in Fig. 1. We, therefore, assume that in the undoped materials $[V_{Br}^{\cdot}]$ is fixed by the oxygen impurity content and that this vacancy concentration is partly compensated by the incorporation of $PbBr_2$ through annihilation of Schottky defects via (1). In all cases the data indicate that $[V_{Br}^{\cdot}]_{\text{oxygen impurities}} > [V_F^{\cdot}]_{\text{excess } PbBr_2}$ holds.

The data in Fig. 2 reveal that the incorporation of AgBr lowers the ionic conductivity with respect to undoped crystals. The effect of an incorporation of AgBr in crystals wherein an extrinsic concentration of bromide ion vacancies is present is similar to that of the incorporation of $PbBr_2$, except for the creation of lead ion vacancies in the latter case. AgBr will be incorporated substitutionally according to

$$AgBr \rightarrow Ag_{Pb}' + V_F^{\cdot} + Br_{Br}^{\times}. \quad (8)$$

This means that the aforementioned oxygen impurities generate not only bromide ion vacancies, but also lead ion vacancies, i.e. reactions (5) and (7) prevail, since only under this condition $[V^{\cdot}_{Br}]$ can decrease upon doping with AgBr through annihilation of Schottky defects via Eq. (1). This is in line with a preferential incorporation of oxide ions on fluoride ion sites. The incorporation scheme presented so far is based on low-temperature conduction governed by bromide ion vacancies. This is not in contradiction with the observation that $t_{F^-} = 1 - t_{Br^-} = 0.87$ (*1*) at elevated temperatures. It has been well established that PbFCl exhibits conduction via $V^{\cdot}_{Cl}$ at low and via $V^{\cdot}_{F}$ at high temperatures (*6*). The great similarity between the crystal structures of PbFCl and PbFBr validates furthermore the aforementioned conduction mechanism for PbFBr.

Doping with LaF_3 is expected to raise the bromide ion vacancy concentration according to

$$LaF_3 \rightarrow La^{\cdot}_{Pb} + 2V''_{Pb} + 3F^{\times}_{F} + 3V^{\cdot}_{Br} \quad (9)$$

and hence the extrinsic conductivity with respect to the undoped starting material. From the data in Fig. 3 it is evident that curves 4 to 7 are in line with this expectation. Curve 3, however, violates this expectation. A comparison between the data in Figs. 2 and 3 reveals that the conductivities ($\| c$-axis) of undoped starting materials originating from different batches spread over almost two decades. Even within one ingot the spread is substantial as is illustrated by the data in Fig. 3. This is inherent to the growth technique employed (*3*). This suggests that variations in the composition of the host lattice are the major cause of the spread in the conductivity data parallel to the c-axis as presented in Fig. 3.

AgF will be incorporated according to

$$AgF \rightarrow Ag'_{Pb} + F^{\times}_{F} + V^{\cdot}_{Br} \quad (10)$$

and should, therefore, increase the extrinsic conductivity. Unfortunately, however, the data presented in Fig. 4 show dissolution of AgF, since up to 400°K the conductivity is independent of the dopant. The obtained value of 0.59 eV for the conductivity activation enthalpy can therefore be used to evaluate the dissolution enthalpy (ΔH_s) of AgF into PbFBr according to reaction (10). This slope represents the value $\Delta H_m + \frac{1}{2}\Delta H_s$, where ΔH_m equals the ΔH_1 (p.c) obtained from polycrystalline materials without AgF-dopant. The experimental data lead to the value of about 1.0 eV for ΔH_s.

Contrary to the results for PbFCl (*3, 6*), we conclude that all the compositions of the various PbFBr samples used in this study are dominated by oxygen impurities. In several samples these impurities are partly compensated by deviations from molecularity. Deliberately added dopants exhibit, due to their low solubilities, in most instances marginal effects on the conductivity.

In order to correlate defect jumps with the observed conductivity activation enthalpies we have presented in Fig. 5 the most likely defect jumps in the unit cell (*6*). The jumps ω_a(Br), ω_d(Br) and ω_3(F) contribute to the conductivity parallel to the crystallographic c-axis. In view of the concentration dependence of the conductivity ΔH_1 and ΔH_2 for conductivity parallel to the c-axis must be correlated with jumps ω_a(Br) and ω_d(Br), respectively. Jump ω_a(Br) contributes to d.c. conductivity by bromide ions, while jump ω_d(Br) contributes to fluoride ion conductivity, since this jump leads to anti-structure defects, according to

$$V^{\cdot}_{Br} + F^{\times}_{F} \rightarrow F^{\times}_{Br} + V^{\cdot}_{F}, \omega_d(Br). \quad (11)$$

The large differences in magnitude of the conductivity associated with ΔH_3 indicate that this is also of an extrinsic nature. In line with the observation that in this region still mixed anionic conduction prevails we propose that jump ω_3(F), i.e.

$$V^{\cdot}_{F} + Br^{\times}_{Br} \rightarrow Br^{\times}_{F} + V^{\cdot}_{Br} \quad (12)$$

contributes to the conductivity in this region. This jump requires the presence of $V^{\cdot}_{F}$ and

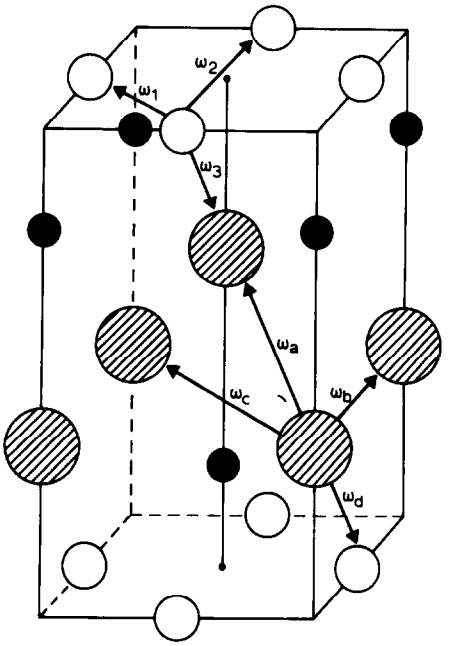

FIG. 5. Unit cell of PbFBr and possible defect jumps. Open circles F, hatched circles Br, and black circles Pb (see text).

possibly V''_{Pb} in the neighborhood of $Br^{\times}_{Br}$, to provide the necessary space to squeeze the fluoride ion layer. As has been shown V''_{Pb} can only be accounted for on the basis of the impurity content. The occurrence of ω_3(F) at elevated temperatures may therefore be regarded as a consequence of the jumps ω_d(Br). Values for ΔH_3 ($\parallel$ c-axis) as presented in Table I are in reasonable agreement. It has to be noted that inhomogeneity of the samples may lead to anomalous conductivity behavior and prevents an accurate determination of ΔH_3. We, therefore, assign a value of about 0.8 eV to jump ω_3(F).

Mass transport in the layers perpendicular to the crystallographic c-axis can occur through jumps ω_1(F) and ω_2(F) in the case of conduction by fluoride ion vacancies, and ω_a(Br), ω_b(Br) and ω_c(Br) in the case of conduction by $V^{\cdot}_{Br}$. From these jumps, ω_2(F) and ω_c(Br) may be ruled out on structural considerations. The value of 0.15 eV for ΔH_1 ($\perp$ c-axis) then should be either associated with jump ω_a(Br) or ω_b(Br). It should be noted that this value is close to the value obtained for ΔH_1 ($\parallel$ c-axis) which was ascribed to jump ω_a(Br). If jump ω_a(Br) were to govern the low-temperature conductivity both parallel and perpendicular to the c-axis, one would expect that $\sigma_{\parallel} \approx \sigma_{\perp}$ (*6*), since this jump has about equal contributions to $\sigma_{\parallel}$ and $\sigma_{\perp}$. In view of the anisotropy of the ionic conductivity (see Fig. 3) we tentatively assign ΔH_1 ($\perp$ c-axis) to jump ω_b(Br).

For ΔH_2 ($\perp$ c-axis) the value of 0.41 eV has been obtained. When jump ω_d(Br) would be involved, the structure of PbFBr suggests that $\sigma_{\parallel} > \sigma_{\perp}$. This is not observed. Therefore, ΔH_2 ($\perp$ c-axis) should be connected with jump ω_1(F). Since we could only measure ΔH_3 ($\perp$ c-axis) for one sample, we cannot be conclusive about the intrinsic or extrinsic nature of this slope. If this part of the curve were to be intrinsic, a value of about 2.1 eV can be extracted from the data for the formation enthalpy ΔH_f of a Schottky defect trio. In the case of PbFCl ΔH_f was estimated to be about 2.6 eV (*6*).

The present assignment of ΔH-values to possible vacancy jumps in the PbFBr lattice is equal to the one presented for PbFCl (*6*).

Acknowledgments

The author is indebted to Drs. G. Calis for assistance in the experiments and to Dr. J. Schoonman and Prof. Dr. G. Blasse for encouraging stimulation and valuable criticism during the preparation of the manuscript.

References

1. LANDOLT-BORNSTEIN, "Zahlenwerte und Funktionen, 6. Aufl., Teil 6, Elektrische Eigenschaften," I, p. 244.
2. W. NIEUWENKAMP AND J. M. BIJVOET, *Z. Krista-llogr.* **82**, 157 (1932).
3. A. F. HALFF AND J. SCHOONMAN, *Z. Phys. Chem.* (N.F.), in press.
4. A. F. CORSMIT AND G. J. DIRKSEN, *J. Crystal Growth* **37**, 187 (1977).

5. A. J. H. EIJKELENKAMP, Thesis, State University of Utrecht, 1976, p. 80.
6. A. F. HALFF AND J. SCHOONMAN, *J. Solid State Chem.*, **27** (1979) in press.
7. A. J. H. EIJKELENKAMP, *Phys. Status. Solidi B* **76**, 153 (1976).
8. W. E. VAN DEN BROM, J. SCHOONMAN, AND J. H. W. DE WIT, *J. Solid State Chem.* **4**, 475 (1972).